



Supplement of

Leveraging machine learning for quantitative precipitation estimation from Fengyun-4 geostationary observations and ground meteorological measurements

Xinyan Li et al.

Correspondence to: Yuanjian Yang (yyj1985@nuist.edu.cn)

The copyright of individual parts of the supplement might differ from the article licence.

1 **Figures and Tables**

2 **Table S1: Classification of rainfall levels in different periods (Unit: mm)**

Level	Rainfall in different periods	
	Rainfall in 1 hours	Rainfall in 24 hours
light rainfall	< 0.1	< 0.1
Light rain	0.1 ~ 1.5	0.1 ~ 9.9
Moderate rain	1.6 ~ 6.9	10.0 ~ 24.9
Heavy rain	7.0 ~ 14.9	25.0 ~ 49.9
Rainstorm	15.0 ~ 39.9	50.0 ~ 99.9
Heavy rainstorm	40.0 ~ 49.9	100.0 ~ 249.9
Extraordinary rainstorm	≥ 50.0	≥ 250.0

3

4

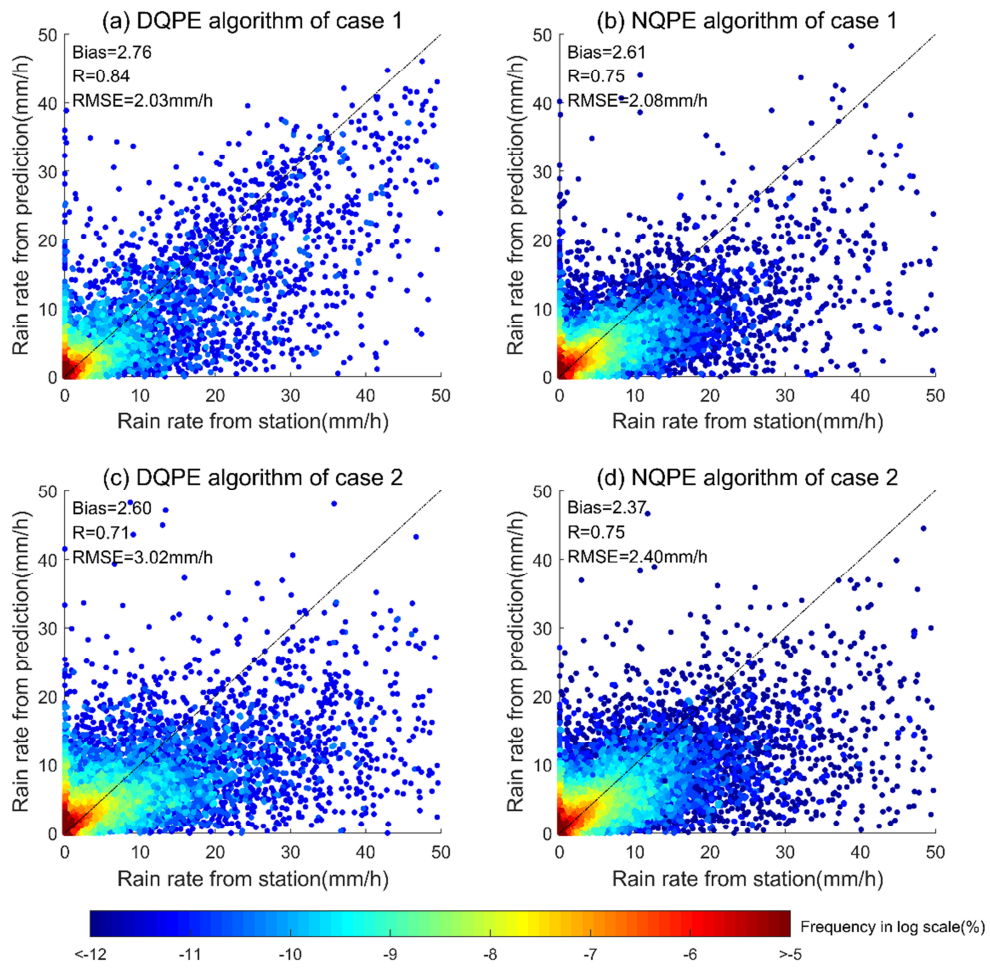
5

6

Table S2: Wavelengths of the 14 channels of the Fengyun-4 satellite and their application

Channel	NO.	Band (μm)	Application
Visible&Near-Infrared	1	0.47	Cloud, Aerosol
	2	0.65	Cloud, Snow
	3	0.825	Cloud, Aerosol, Vegetation
	4	1.375	Cirrus
	5	1.61	Cloud, Snow
	6	2.25	Cirrus, Aerosol
Shortwave Infrared	7	3.75H	Fire
	8	3.75L	Clouds, Fog
Water Vapor	9	6.25	WV
	10	7.1	WV
Longwave Infrared	11	8.5	Sand dust
	12	10.7	Cloud
	13	12.0	Cloud
	14	13.5	Cloud

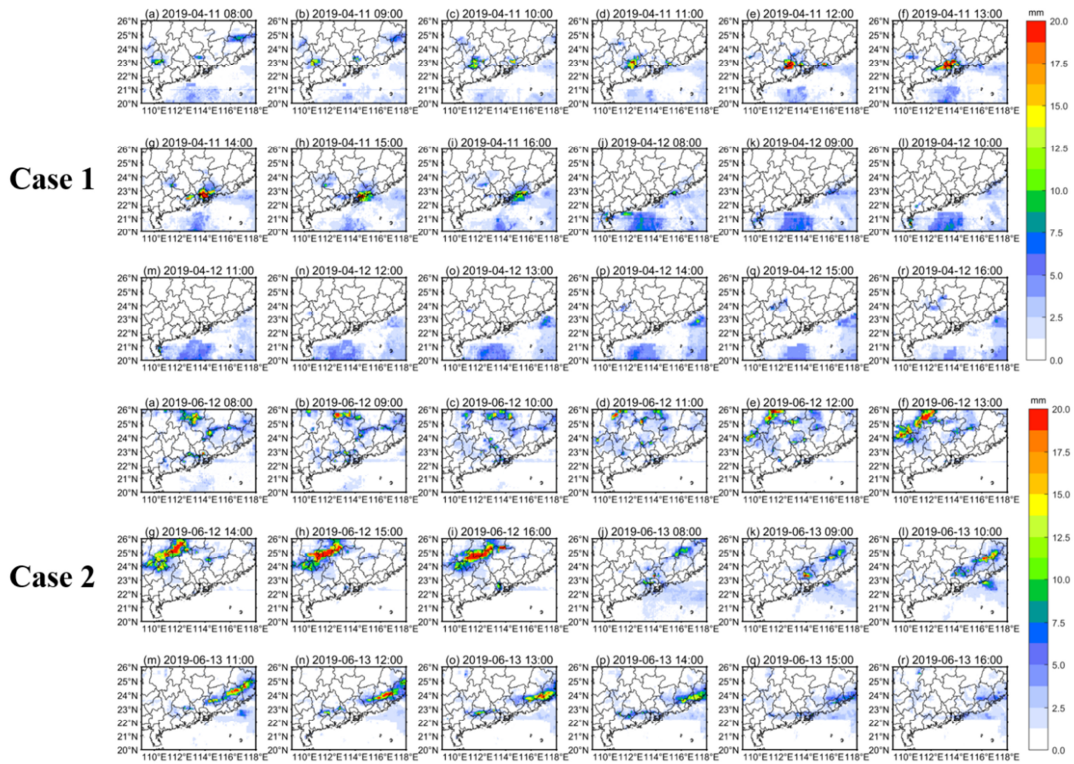
7



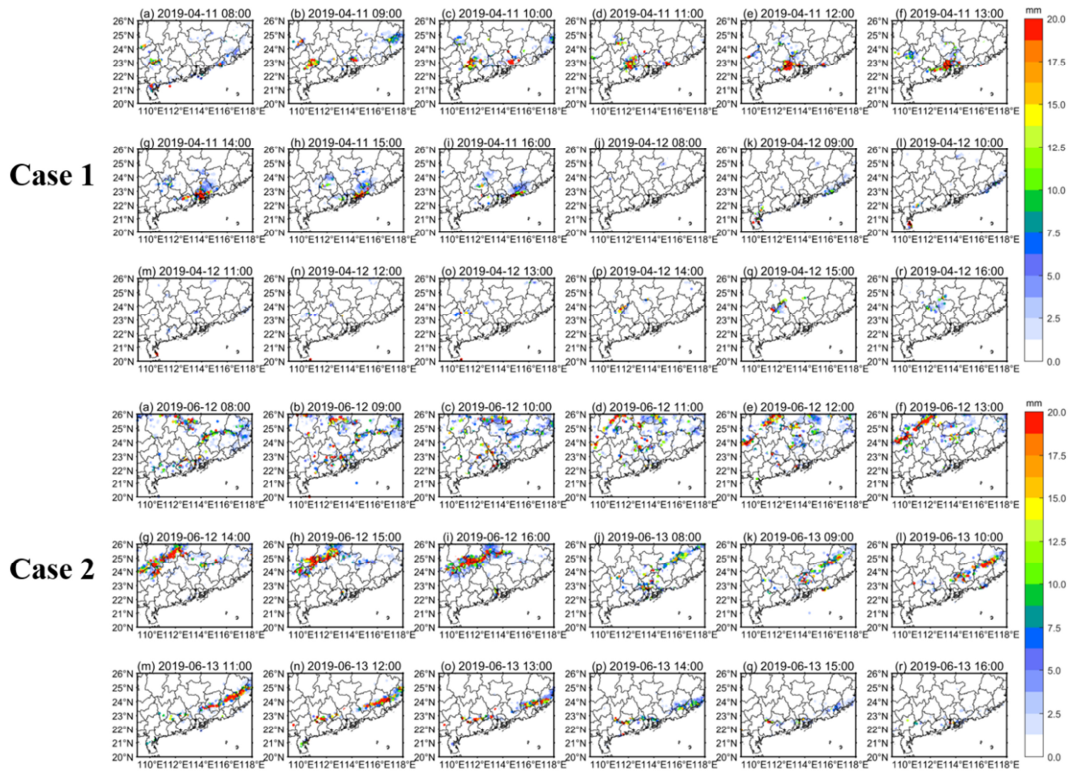
8

9 **Figure S1: Comparison of the precipitation measured by high-density automatic stations and that estimated by**
 10 **the QPE algorithm: (a) DQPE algorithm of case 1; (b) NQPE algorithm of case 1; (c) DQPE algorithm of case 2;**
 11 **(d) NQPE algorithm of case 2**

12

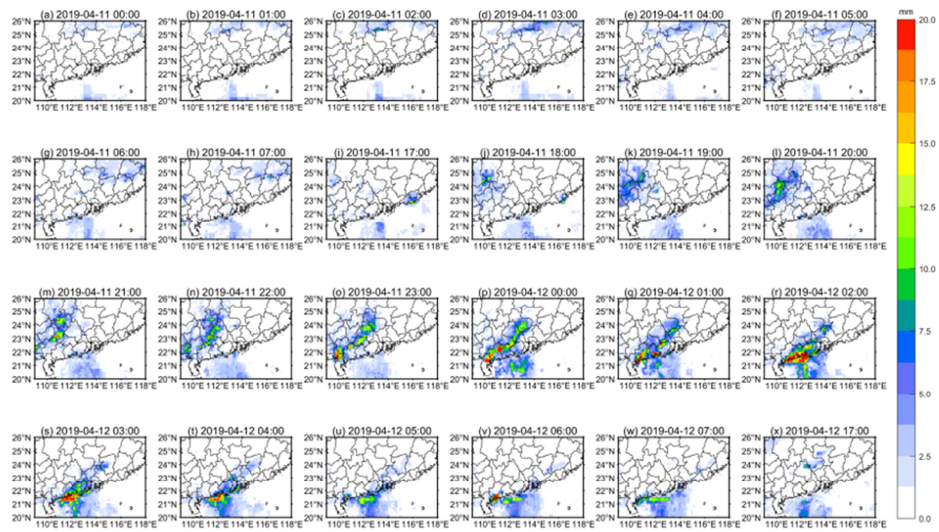


15 **Figure S2: Estimated precipitation of the DQPE algorithm: Case 1: (a–i) at 0800–1600 BJT on April 11; (j–r) at**
 16 **0800–1600 BJT on April 12. Case 2: (a–i) at 0800–1600 BJT on June 12; (j–r) at 0800–1600 BJT on June 13.**

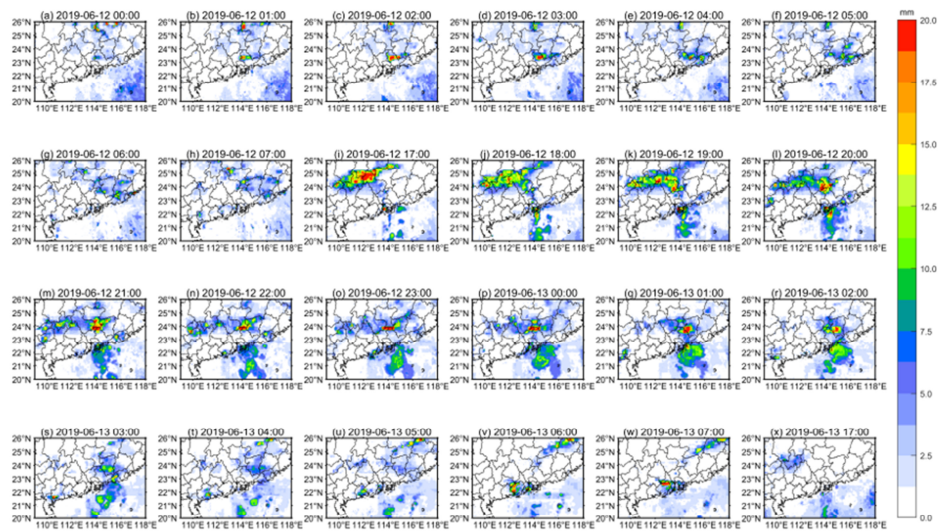


20 **Figure S3: Actual precipitation based on the high-density automatic stations: Case 1: (a–i) at 0800–1600 BJT on**
 21 **April 11; (j–r) at 0800–1600 BJT on April 12. Case 2: (a–i) at 0800–1600 BJT on June 12; (j–r) at 0800–1600 BJT**
 22 **on June 13.**

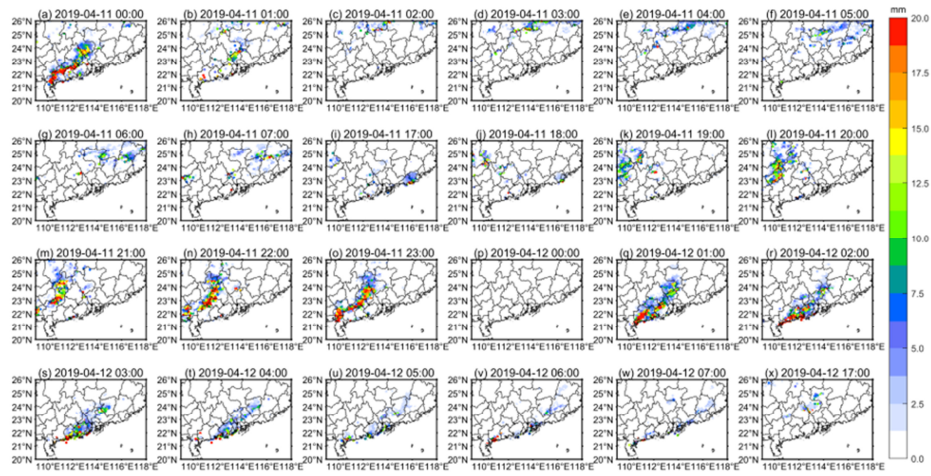
Case 1



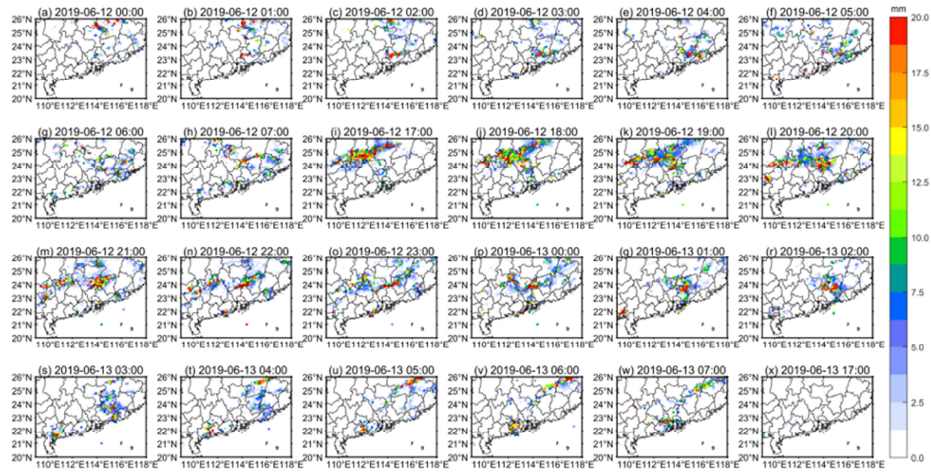
Case 2



Case 1

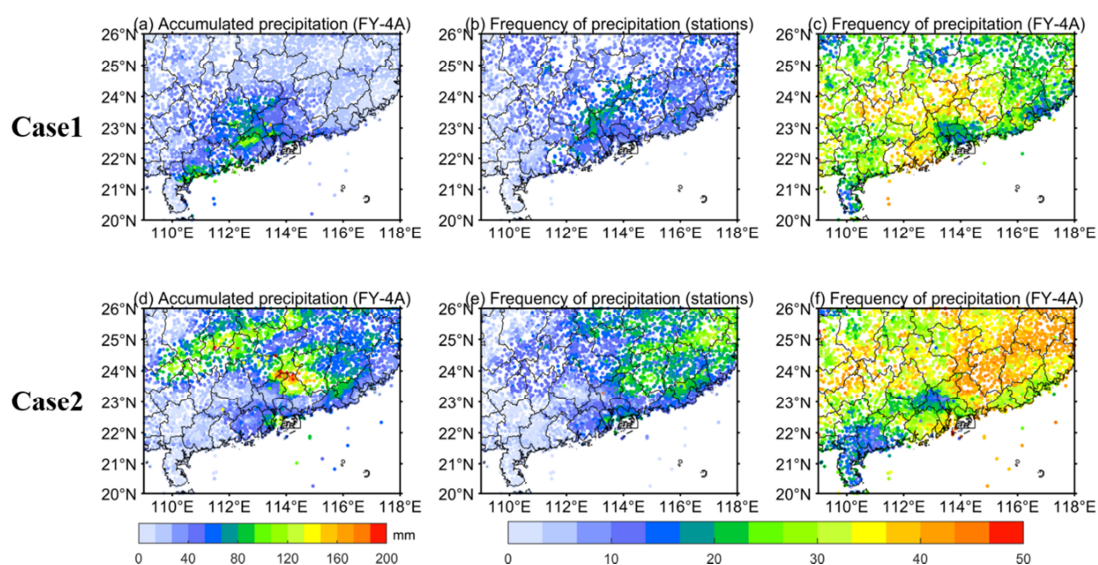


Case 2



33 **Figure S5: Actual precipitation based on the high-density automatic stations: Case 1: (a–h) 0000–0700 BJT on**
 34 **April 11, (i–o) 1700–2300 BJT on April 11, (p–w) 0000–0700 BJT on April 12, and (x) 1700 BJT on April 12.**

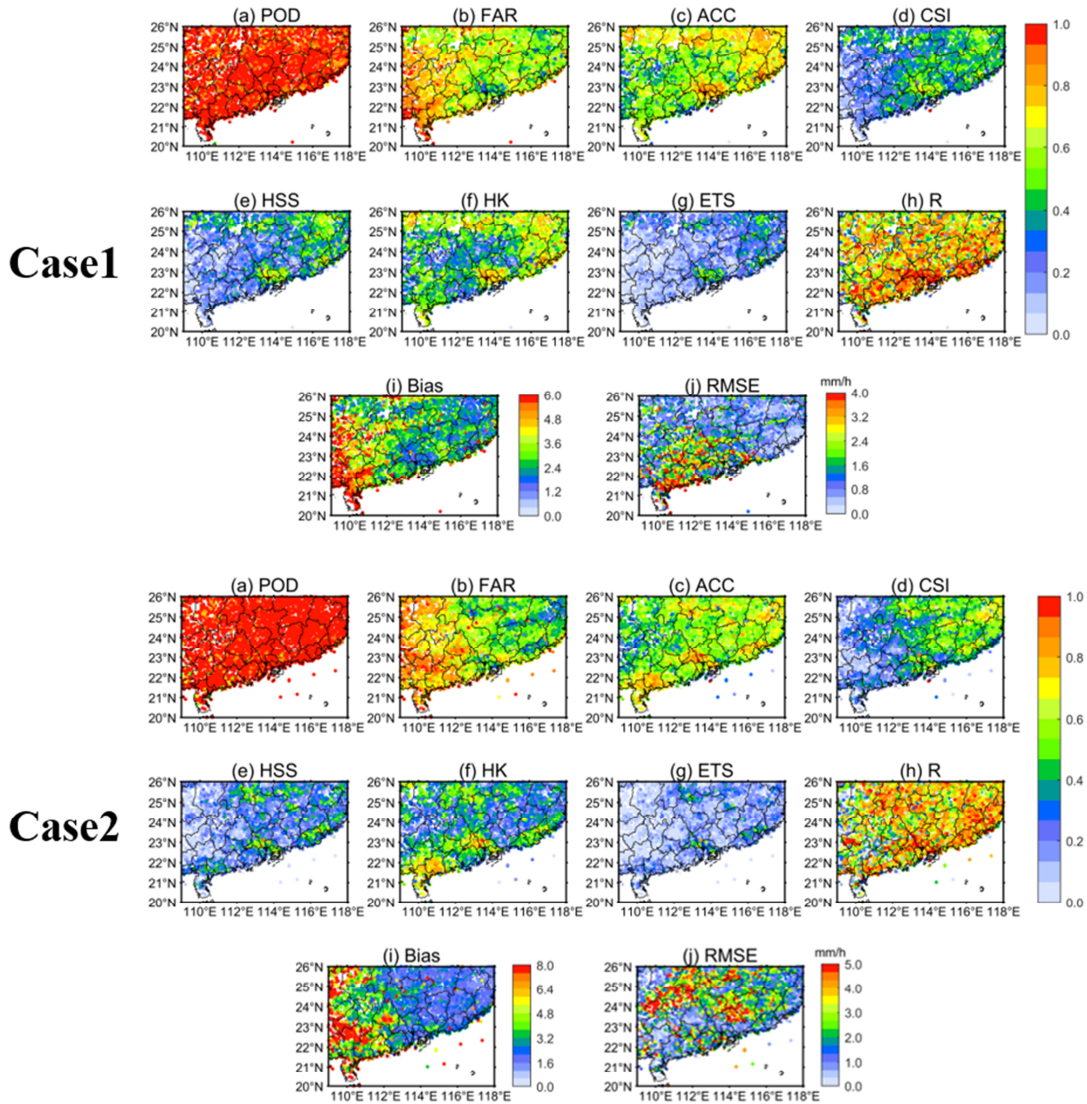
35 **Case 2: (a–h) 0000–0700 BJT on June 12, (i–o) 1700–2300 BJT on June 12, (p–w) 0000–0700 BJT on June 13,**
 36 **and (x) 1700 BJT on June 13.**



39

40 **Figure S6: Spatial distribution of accumulated precipitation: (a) accumulated precipitation estimated by the**
 41 **QPE algorithm in case 1; (b) actual precipitation frequency observed by high-density automatic stations in case**
 42 **1; (c) precipitation frequency estimated by the QPE algorithm in case 1; (d) accumulated precipitation estimated**
 43 **by the QPE algorithm in case 2; (e) actual precipitation frequency observed by high-density automatic stations**
 44 **in case 2; (f) precipitation frequency estimated by the QPE algorithm in case 2.**

45

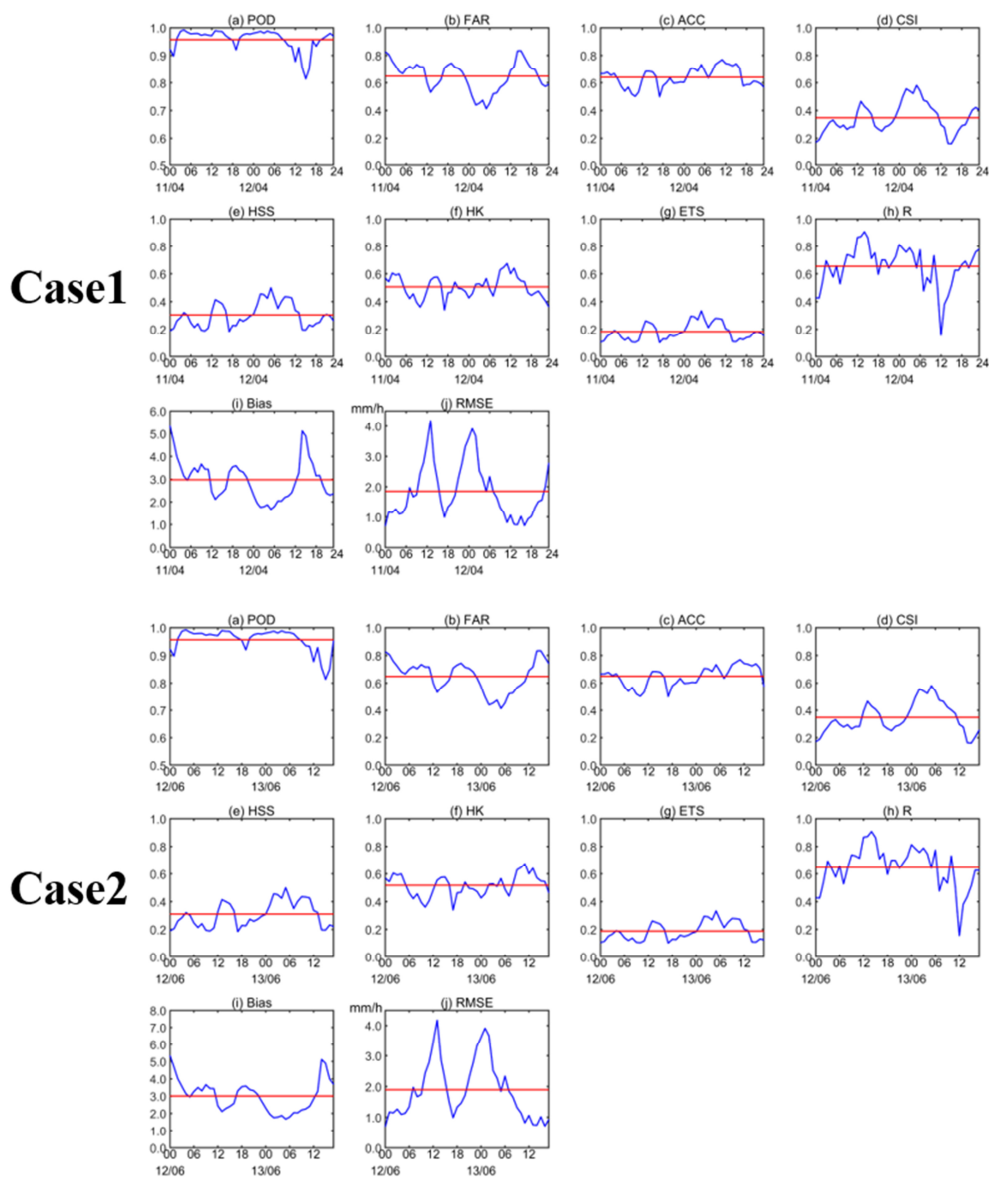


47

48 **Figure S7: Spatial distribution of evaluation indicators of the QPE algorithm for all stations: Case 1: (a) *POD*; (b)**
 49 ***FAR*; (c) *ACC*; (d) *CSI*; (e) *HSS*; (f) *HK*; (g) *ETS*; (h) *R*; (i) *Bias*; (j) *RMSE*. Case 2:(a) *POD*; (b) *FAR*; (c) *ACC*;**
 50 ***(d) *CSI*; (e) *HSS*; (f) *HK*; (g) *ETS*; (h) *R*; (i) *Bias*; (j) *RMSE*.***

51

52



54

55 **Figure S8: Time series of evaluation indicators of the QPE algorithm for all stations at each time: Case 1: (a)**56 ***POD*; (b) *FAR*; (c) *ACC*; (d) *CSI*; (e) *HSS*; (f) *HK*; (g) *ETS*; (h) *R*; (i) *Bias*; (j) *RMSE*. Case 2:(a) *POD*; (b) *FAR*;**57 **(c) *ACC*; (d) *CSI*; (e) *HSS*; (f) *HK*; (g) *ETS*; (h) *R*; (i) *Bias*; (j) *RMSE*.**

58